RESEARCH ARTICLE SUMMARY

NEURODEVELOPMENT

Cortical wiring by synapse type–specific control of local protein synthesis

Clémence Bernard, David Exposito-Alonso†, Martijn Selten†, Stella Sanalidou, Alicia Hanusz-Godoy, Alfonso Aguilera, Fursham Hamid, Fazal Oozeer, Patricia Maeso, Leanne Allison, Matthew Russell, Roland A. Fleck, Beatriz Rico*, Oscar Marín*

INTRODUCTION: The function of the cerebral cortex relies on the specificity of synaptic connections among dozens of different types of excitatory glutamatergic pyramidal cells and inhibitory γ-aminobutyric acid-containing (GABAergic) interneurons. Neurons use dedicated transcriptional programs to control synapse specificity during development. Still, it is presently unclear whether regulation of mRNA translation is also involved in promoting the formation of specific synapses. One of the main signaling pathways controlling protein synthesis involves the mechanistic target of rapamycin complex 1 (mTORC1), a molecular complex activated by growth factor signals and inhibited by the proteins Tsc1 and Tsc2 (TSC subunits 1 and 2, respectively). Multiple proteins of the mTORC1 pathway are present in developing axons, and local protein synthesis occurs at excitatory and inhibitory synapses in the adult cerebral cortex. Many genes whose variation has been linked to neurodevelopmental disorders code proteins found at synapses and altered protein synthesis is a plausible pathophysiological mechanism for several of these conditions. For example, mutations in *TSC1* and *TSC2* cause tuberous sclerosis, a syndrome whose clinical features include seizures and autism spectrum disorder (ASD).

RATIONALE: Local translation contributes to brain wiring during axon guidance but its direct contribution to synapse formation is unclear. Moreover, to what extent local translation is differentially regulated at the level of specific synaptic connections remains unknown. We used mouse genetics, RNA sequencing, biochemistry, and experimental manipulations in vivo to study local protein synthesis in the development of synaptic connections in the cerebral cortex. We investigated the formation of excitatory synaptic connections between cortical pyramidal cells and two of the main subclasses of cortical interneurons, parvalbumin (PV)- and somatostatin (SST)-expressing cells. These interneurons share similar developmental trajectories, occupy the same layers of the neocortex, and are reciprocally connected with pyramidal cells, but they play very different roles in cortical function.

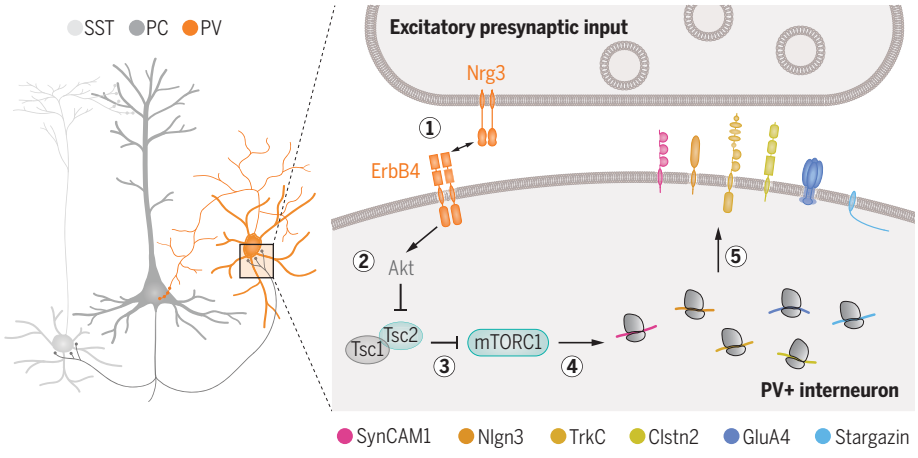

Local protein synthesis in synapse formation. Schematic of a pyramidal cell contacting parvalbumin-expressing (PV+) and somatostatin-expressing (SST+) interneurons in the cerebral cortex. The development of excitatory synapses on PV+ interneurons is mediated by (**1**) activation of ErbB4 through binding to neuregulin 3 (Nrg3) expressed by pyramidal cells, (**2**) inhibition of Tsc2 through Akt-dependent phosphorylation cascade, (**3**) inhibition of mTORC1 through Rheb-dependent phosphorylation cascade, (**4**) activation of protein synthesis of ErbB4 targets at the synapse, and (**5**) synapse formation through ErbB4 targets.

RESULTS: We found that loss of Tsc2 during development causes overactivation of mTORC1 in both PV^+ and SST^+ interneurons, leading to abnormal activation of mTORC1 effector protein S6rp and increased cell size. However, Tsc2 function seems required to establish a normal complement of excitatory synapses only onto PV^+ and not SST^+ interneurons. Tsc2 also seems dispensable for developing inhibitory PV^+ synapses onto pyramidal cells. Thus, although the loss of Tsc2 causes a global disruption of mTOR signaling in both PV^+ and SST^+ cells, it affects the wiring of interneurons in a cell type–specific and synapse type–specific manner. Our experiments indicate that this specificity is mediated by the Erb-B2 receptor tyrosine kinase 4 (ErbB4), which is specifically expressed by PV^+ interneurons and is present at postsynaptic densities contacted by excitatory axons. ErbB4 signaling inhibits Tsc2 function to enable mTOR activity at the postsynaptic densities of excitatory inputs contacting PV^+ interneurons. ErbB4 activation ultimately leads to the synaptic translation of mRNAs coding cell adhesion molecules (SynCAM1, Nlgn3, TrkC, and Clstn2) and AMPA receptor-related proteins (GluA4 and Stargazin). Loss of function experiments revealed that these molecules are required to develop a normal complement of excitatory synapses on PV^+ interneurons. Although a direct link between ErbB4 activation and local protein synthesis has only been established for a few mRNAs, analysis of the synaptic translatome of PV^+ interneurons lacking ErbB4 suggests that local translation of more transcripts—including many for which variation has been associated with ASD—might be under the control of this signaling pathway during synapse formation.

CONCLUSION: Our findings reveal that protein synthesis is regulated in a cell type–specific and synapse type–specific manner during synapse formation. Tsc2, a regulator of mTORC1 signaling in multiple cellular contexts, regulates the development of excitatory synapses onto PV^+ cells but not onto SST^+ interneurons. This specificity is mediated by activation of ErbB4, which controls excitatory synapse development through inhibition of Tsc2 and subsequent induction of a molecular program of local mRNA translation. Thus, local protein synthesis is regulated at the level of specific connections to control synapse formation in the nervous system. ■

The list of author affiliations is available in the full article online.
*Corresponding author. Email: beatriz.rico@kcl.ac.uk (B.R.); oscar.marin@kcl.ac.uk (O.M.)
†These authors contributed equally to this work.
Cite this article as C. Bernard *et al.*, *Science* **378**, eabm7466 (2022). DOI: 10.1126/science.abm7466

RESEARCH ARTICLE

NEURODEVELOPMENT

Cortical wiring by synapse type–specific control of local protein synthesis

Clémence Bernard[1,2], David Exposito-Alonso[1,2]†, Martijn Selten[1,2]†, Stella Sanalidou[1,2], Alicia Hanusz-Godoy[1,2], Alfonso Aguilera[1,2], Fursham Hamid[1,2], Fazal Oozeer[1,2], Patricia Maeso[1,2], Leanne Allison[3], Matthew Russell[3], Roland A. Fleck[3], Beatriz Rico[1,2]*, Oscar Marín[1,2]*

Neurons use local protein synthesis to support their morphological complexity, which requires independent control across multiple subcellular compartments up to the level of individual synapses. We identify a signaling pathway that regulates the local synthesis of proteins required to form excitatory synapses on parvalbumin-expressing (PV^+) interneurons in the mouse cerebral cortex. This process involves regulation of the TSC subunit 2 (Tsc2) by the Erb-B2 receptor tyrosine kinase 4 (ErbB4), which enables local control of messenger RNA {mRNA} translation in a cell type–specific and synapse type–specific manner. Ribosome-associated mRNA profiling reveals a molecular program of synaptic proteins downstream of ErbB4 signaling required to form excitatory inputs on PV^+ interneurons. Thus, specific connections use local protein synthesis to control synapse formation in the nervous system.

The diversity of animal behaviors relies on the precise assembly of neuronal circuits, a process in which synapse formation plays a role. In the cerebral cortex, dozens of different types of excitatory glutamatergic pyramidal cells and inhibitory γ-aminobutyric acid-containing (GABAergic) interneurons are wired through distinct connectivity motifs (*1*, *2*). For example, layer 4 excitatory neurons receive inputs from excitatory thalamic neurons and project to layer 2/3 excitatory neurons and feedforward interneurons (*3*). Synapse specificity is established during development by dedicated transcriptional programs (*4*–*10*), but whether regulation of mRNA translation is also involved in this process remains to be elucidated.

Several pathways control protein synthesis (*11*, *12*), including the mechanistic target of rapamycin complex 1 (mTORC1), a molecular complex composed of mTOR kinase and several other proteins, which is activated by nutrients and growth factor signals and inhibited by the proteins Tsc1 and Tsc2 (*13*, *14*). Multiple mTORC1 pathway proteins and the translation machinery have been identified in developing axons (*15*–*17*), and local protein synthesis occurs at excitatory and inhibitory synapses in the adult brain (*18*–*24*). To what extent local translation is differentially regulated in closely related cell types and at the level of specific synapses during the wiring of cortical circuits is unknown.

[1]Centre for Developmental Neurobiology, Institute of Psychiatry, Psychology and Neuroscience, King's College London, London SE1 1UL, UK. [2]MRC Centre for Neurodevelopmental Disorders, King's College London, London SE1 1UL, UK. [3]Centre for Ultrastructural Imaging, King's College London, London SE1 1UL, UK.
*Corresponding author. Email: beatriz.rico@kcl.ac.uk (BR); oscar.marin@kcl.ac.uk (OM)
†These authors contributed equally to this work.

Specific synaptic defects in interneurons lacking Tsc2

To explore the role of protein synthesis in the wiring of different cell types in the cerebral cortex, we generated mice in which we deleted *Tsc2* from the two largest groups of cortical GABAergic interneurons: parvalbumin (PV)- and somatostatin (SST)-expressing cells. To this end, we crossed *Lhx6-Cre* mice, which drives recombination in early postmitotic PV^+ and SST^+ interneurons, with mice carrying conditional (i.e., Cre-dependent) *Tsc2* alleles ($Tsc2^{F/F}$) and a reporter for the visualization of recombined cells (see Methods). We chose these two cell types because although they derive from common progenitors in the medial ganglionic eminence (MGE) and the preoptic area (POA), populate the same layers of the neocortex, and are both reciprocally connected with pyramidal cells (*25*), they play very different roles in cortical information processing (*26*). We first confirmed that loss of *Tsc2* (fig. S1, A and B) leads to overactivation of mTOR signaling in PV^+ and SST^+ interneurons by analyzing the levels of phosphorylated S6 ribosomal protein (P-S6rp), a critical downstream effector of mTORC1 (*12*). We observed increased levels of P-S6rp in conditional *Tsc2* mutants compared with controls (fig. S1, C and D). We also found that the cell size of PV^+ and SST^+ interneurons is larger in conditional *Tsc2* mutants than in controls (fig. S1, C and E), reinforcing the notion that mTOR signaling is indeed overactive in these cells (*27*, *28*). Consistent with a previous report (*29*), we also noticed an increased density in an infrequent population of cortical interneurons that coexpress PV^+ and SST^+ in conditional *Tsc2* mutants compared with controls (fig. S2). By contrast, *Tsc2* loss does not affect the density or laminar distribution of PV^+ and SST^+ interneurons (fig. S2).

We next investigated whether loss of Tsc2 affects synapse formation onto PV^+ and SST^+ interneurons in the neocortex. To this end, we assessed the number of excitatory synapses received by cortical PV^+ and SST^+ interneurons by quantifying puncta containing vesicular glutamate transporter 1 (VGluT1), a characteristic component of excitatory glutamatergic terminals, and PSD95, the primary scaffolding protein in the excitatory postsynaptic density, on the soma and dendrites of PV^+ and SST^+ interneurons (Fig. 1 and fig. S3). We found that the loss of one and, even more so, two *Tsc2* alleles in PV^+ interneurons led to an increase in the density of excitatory synapses received by these cells compared with control littermates (Fig. 1, A and B, and fig. S3, A and B). By contrast, conditional deletion of *Tsc2* caused no changes in the density of excitatory synapses received by SST^+ interneurons (Fig. 1, C and D, and fig. S3C). The size of $VGluT1^+$ boutons and $PSD95^+$ puncta was not altered by the loss of Tsc2 (fig. S4).

To explore whether the supernumerary excitatory synapses contacting PV^+ interneurons in conditional *Tsc2* mutants represent functional synapses, we analyzed synaptic function by whole-cell recordings. Analysis of miniature excitatory postsynaptic currents (mEPSCs) revealed no differences in the frequency or amplitude of these synaptic events between control and conditional *Tsc2* mutants (fig. S5, A to E), which indicated that the supernumerary excitatory synapses contacting PV^+ interneurons lacking Tsc2 could either have altered release properties or be functionally inactive. To distinguish between both possibilities, we assessed release probability by recording paired-pulse ratios in PV^+ interneurons and found no differences between both genotypes (fig. S5, F and G). These observations suggested that the supernumerary excitatory synapses decorating PV^+ interneurons in conditional *Tsc2* mutants might not be mature.

We also observed cell type–specific alterations in intrinsic properties following the conditional deletion of *Tsc2* (fig. S6A). These changes led to a reduction in the excitability of PV^+ interneurons in conditional *Tsc2* mutants compared with controls, whereas no difference was observed for SST^+ interneurons (fig. S6B). Finally, the differential impact of the loss of Tsc2 in the integration of PV^+ and SST^+ interneurons in cortical networks was examined by recording spontaneous excitatory postsynaptic currents (sEPSCs) in both cell types (Fig. 1E). *Tsc2*

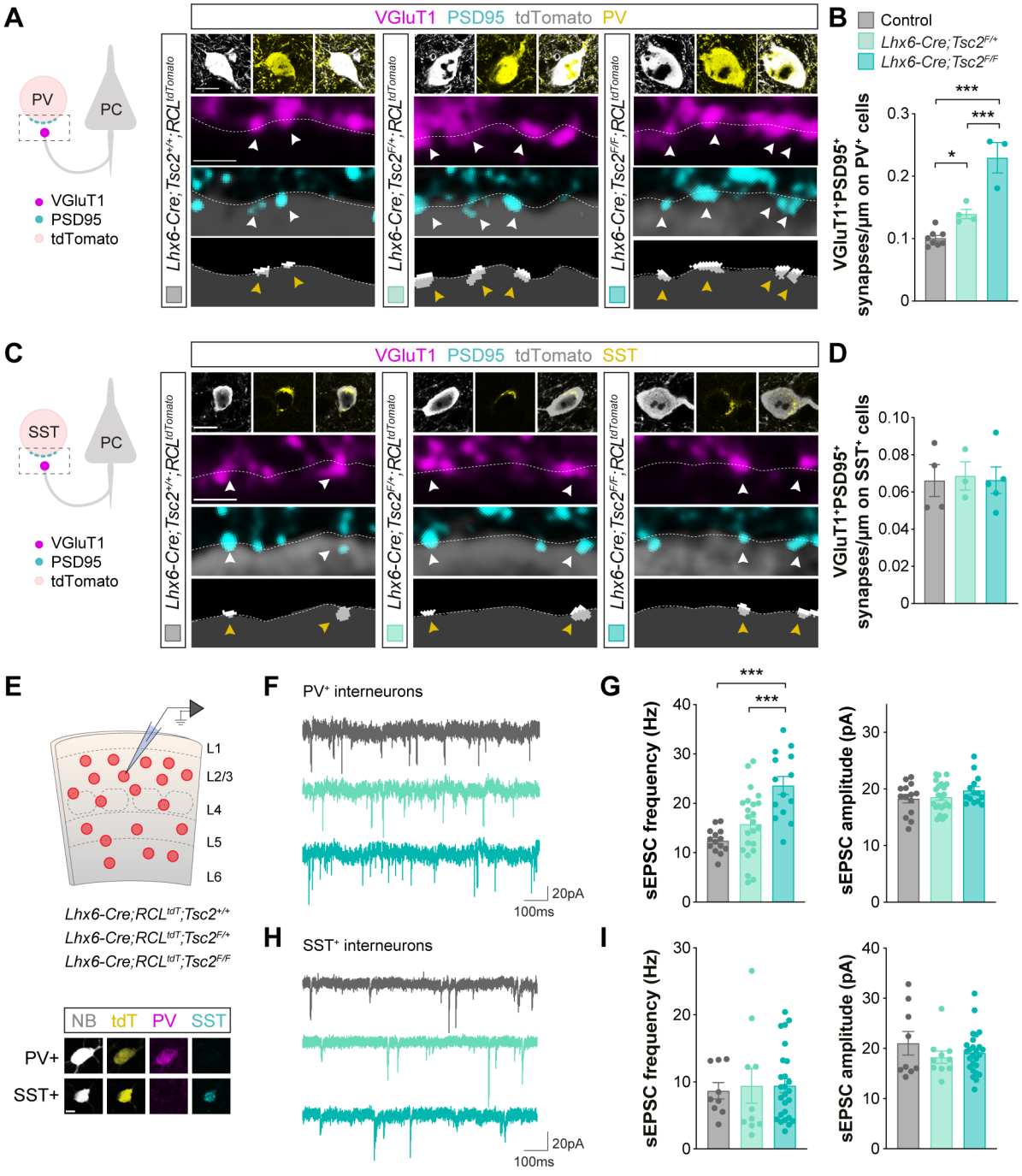

Fig. 1. Differential contribution of Tsc2 to synapse development.
(**A**) Schematic of synaptic markers analyzed (left). Confocal images (top) and binary images (bottom) illustrating presynaptic VGluT1$^+$ puncta (magenta) and postsynaptic PSD95$^+$ clusters (cyan) in PV$^+$ (yellow) tdTomato$^+$ (gray) interneurons from P18-21 control, heterozygous and homozygous conditional *Tsc2* mutants. (**B**) Quantification of the density of VGluT1$^+$PSD95$^+$ synapses contacting PV$^+$ interneurons (control, *n* = 111 cells from 8 mice; heterozygous, *n* = 70 cells from 4 mice; homozygous, *n* = 46 cells from 3 mice). (**C**) Schematic of synaptic markers analyzed (left). Confocal images (top) and binary images (bottom) illustrating presynaptic VGluT1$^+$ puncta (magenta) and postsynaptic PSD95$^+$ clusters (cyan) in SST$^+$ (yellow) tdTomato$^+$ (gray) interneurons from P18-21 control, heterozygous and homozygous conditional *Tsc2* mutants. (**D**) Quantification of the density of VGluT1$^+$PSD95$^+$ synapses contacting SST$^+$ interneurons (control, *n* = 67 cells from 4 mice; heterozygous, *n* = 41 cells from 3 mice; homozygous, *n* = 60 cells from 5 mice). (**E**) Schematic of experimental design (top) and post-recording labeling of neurobiotin (NB, gray)-filled tdTomato$^+$ (yellow) cells with PV (magenta) and SST (cyan) (bottom). (**F**) Example traces of sEPSCs recorded from PV$^+$ interneurons from P18-21 control, heterozygous and homozygous conditional *Tsc2* mutants. (**G**) Quantification of the frequency (left) and amplitude (right) of sEPSCs from PV$^+$ interneurons (control *n* = 14 cells from 5 mice, *Lhx6-Cre;Tsc2*$^{F/+}$ *n* = 23 cells from 8 mice, *Lhx6-Cre;Tsc2*$^{F/F}$ *n* = 14 cells from 6 mice). (**H**) Example traces of sEPSCs recorded from SST$^+$ interneurons from P18-21 control, heterozygous, and homozygous conditional *Tsc2* mutants. (**I**) Quantification of the frequency (left) and amplitude (right) of sEPSCs from SST$^+$ interneurons (control, *n* = 9 cells from 5 mice; heterozygous, *n* = 10 cells from 9 mice;

homozygous, n = 26 cells from 7 mice). One-way ANOVA followed by Tukey's multiple comparisons test or Kruskal-Wallis followed by Dunn's multiple comparisons test: *P < 0.05, **P < 0.01, ***P < 0.001. The dashed lines in the images shown in (A) and (C) outline the surface of the cells. Data are mean ± SEM. Scale bar, 10 μm and 1 μm (high magnification) (A and C), and 10 μm (E).

deletion in PV$^+$ interneurons led to a significant increase in the frequency of sEPSCs with no changes in amplitude (Fig. 1, F and G) whereas neither the frequency nor the amplitude of sEPSCs changed in SST$^+$ interneurons lacking *Tsc2* (Fig. 1, H and I). Altogether, these results revealed that loss of *Tsc2* differentially affects the wiring of PV$^+$ and SST$^+$ interneurons, suggesting a cell type–specific role for Tsc2 in synapse formation.

We next wondered whether the function of Tsc2 in synapse development might be synapse type-specific. We reasoned that if Tsc2 plays a role in synapse formation in PV$^+$ interneurons, loss of Tsc2 should also affect the development of the synapses made by these cells onto pyramidal cells. We focused on PV$^+$ basket cell synapses, which target the soma of pyramidal cells and can be identified by the presynaptic expression of synaptotagmin-2 (Syt2) and gephyrin (Geph), a postsynaptic scaffolding protein of GABAergic synapses (*30*). We found no differences in the density of Syt2$^+$Geph$^+$ synaptic puncta contacting the soma of pyramidal cells in conditional *Tsc2* mutants compared with control littermates (fig. S7). Thus, although the loss of Tsc2 causes a global disruption of mTOR signaling in PV$^+$ and SST$^+$ cells (e.g., increased cell size and P-S6rp), it seems to affect the wiring of interneurons in a cell type–specific and synapse type–specific manner.

Tsc2 functions downstream of ErbB4 in synapses

Because the loss of Tsc2 function leads only to changes in the excitatory synaptic input of PV$^+$ interneurons, we reasoned that Tsc2 activity could be regulated locally by a signaling pathway specific to these synapses and necessary for their formation. In other cellular contexts, Tsc2 activity is inhibited by factors that stimulate cell growth through the phosphorylation of Akt (*14*, *31*). The receptor tyrosine kinase ErbB4—which is enriched in PV$^+$ but not SST$^+$ interneurons and is required for the formation of excitatory synapses onto PV$^+$ interneurons (*32*–*34*)—activates Akt through PI3K phosphorylation (*35*), and associates with Tsc2 in synaptosome preparations obtained from the mouse neocortex during synaptogenesis (fig. S8). This led us to hypothesize that ErbB4 functions upstream of Tsc2 to regulate its activity during the development of these specific synapses (Fig. 2A). To begin testing this hypothesis, we analyzed Tsc2 phosphorylation in synaptosomes obtained from the neocortex of control and interneuron-specific *Erbb4* conditional mutants (Fig. 2B). These preparations are enriched in synaptosomes (fig. S9, A and B), which are predominantly bipartite (fig. S9, C and D, and fig. S10), have both the pre- and postsynaptic sides enclosed in a membrane (fig. S9, E and F, fig. S11) and contain synaptic proteins (fig. S9G). We found reduced Akt-mediated phosphorylation of Tsc2 in cortical synapses from *Erbb4* conditional mutants compared with controls (Fig. 2, C and D). We also found reduced phosphorylation of the mTORC1 effectors S6rp and eIF4E-binding protein 1 (4E-BP1) in synaptosomes from *Erbb4* conditional mutants (Fig. 2, C and D), which indicates that the loss of ErbB4 function decreases mTORC1 synaptic activity as a result of the overactivation of Tsc2. None of these changes were observed in cytosolic fractions (Fig. 2, E and F), suggesting that ErbB4 is required to modulate Tsc2 signaling specifically at the synapse.

We next investigated whether the mTORC1 inactivation observed in *Erbb4* conditional mutants occurs at specific cortical synapses. Because ErbB4 is only expressed by specific classes of interneurons in the cerebral cortex (*32*, *36*), we hypothesized that changes would be limited to synapses that contain ErbB4 receptors, such as the excitatory synapses received by PV$^+$ basket cells. To test this idea, we isolated and plated cortical synaptosomes and analyzed the phosphorylation of S6rp in postsynaptic structures identified with PSD95. We identified excitatory synapses onto inhibitory neurons using neuregulin 3 (Nrg3), a marker of presynaptic excitatory terminals contacting PV$^+$ interneurons (*37*, *38*). We found decreased P-S6rp specifically in Nrg3$^+$/PSD95$^+$ synaptosomes from *Erbb4* conditional mutants compared with controls, but no difference in ErbB4-independent glutamatergic synaptosomes (Fig. 2, G to I) or Syt2$^+$/Geph$^+$ synaptosomes (fig. S12), which correspond to the synapses made by PV$^+$ basket cells onto pyramidal cells. These results indicate that ErbB4 regulates mTOR signaling in excitatory synapses received by PV$^+$ interneurons.

To further support the idea that ErbB4 and Tsc2 function in the same signaling pathway controlling the formation of excitatory synapses onto PV$^+$ cells, we performed a genetic interaction experiment. We generated *Erbb4* conditional mutants carrying a conditional *Tsc2* allele to compromise the function of Tsc2 in PV$^+$ interneurons lacking ErbB4 and measured the density of excitatory synapses received by these cells. We found that deleting one *Tsc2* allele from PV$^+$ cells is sufficient to rescue the loss of excitatory synapses found in *Erbb4* conditional mutants (fig. S13). Altogether, these results demonstrate that Tsc2 functions downstream of ErbB4 in regulating the excitatory synaptic input of PV$^+$ interneurons.

Changes in the synaptic translatome of *Erbb4* mutants

To identify the specific targets of ErbB4 that are involved in the development of synapses in PV$^+$ interneurons, we first obtained the synaptic translatome of MGE/POA-derived interneurons from control and *Erbb4* conditional mutants. To this end, we bred into these mice alleles carrying a mutation in the locus encoding the ribosomal protein L22 (Rpl22) that allows the conditional tagging of ribosomes with a hemagglutinin epitope (HA) tag (*39*). We then prepared synaptosomes from the neocortex of P15 mice, pulled down ribosomes from this preparation using anti-HA beads to isolate ribosome-associated mRNA transcripts from MGE/POA-derived interneurons in control and *ErbB4* conditional mutants, and then analyzed them by RNA sequencing (Fig. 3A and fig. S14, A to D).

We found that 70% of the differentially expressed genes were down-regulated in *Erbb4* conditional mutants compared with controls (Fig. 3B and fig. S14D). Among the down-regulated genes, we observed a significant enrichment in genes associated with autism spectrum disorder (ASD) (fig. S15). Gene ontology (GO) analysis revealed an enrichment in genes involved in processes such as "synapse organization", "neurotransmitter receptor activity", and "glutamatergic synapse" (Fig. 3C and fig. S14E), highlighting synaptic alterations in *Erbb4* conditional mutants. We then identified genes coding for proteins with postsynaptic localization and/or function using synaptic GO annotations (*40*). This analysis revealed that within the postsynaptic category, the most enriched terms were postsynaptic specialization and postsynaptic membrane and, more specifically, genes encoding cell adhesion molecules and AMPA receptors (Fig. 3, D and E, and fig. S14F). Using a set of four additional criteria (see Methods), including their relative enrichment in PV$^+$ cells, we selected seven candidates for functional validation: five cell adhesion molecules, SynCAM1 (encoded by *Cadm1*), Nptn, Nlgn3, TrkC (encoded by *Ntrk3*), and Clstn2, and two AMPA receptor-related proteins, GluA4 (encoded by *GriA4*) and Stargazin (encoded by *Cacng2*) (Fig. 3E).

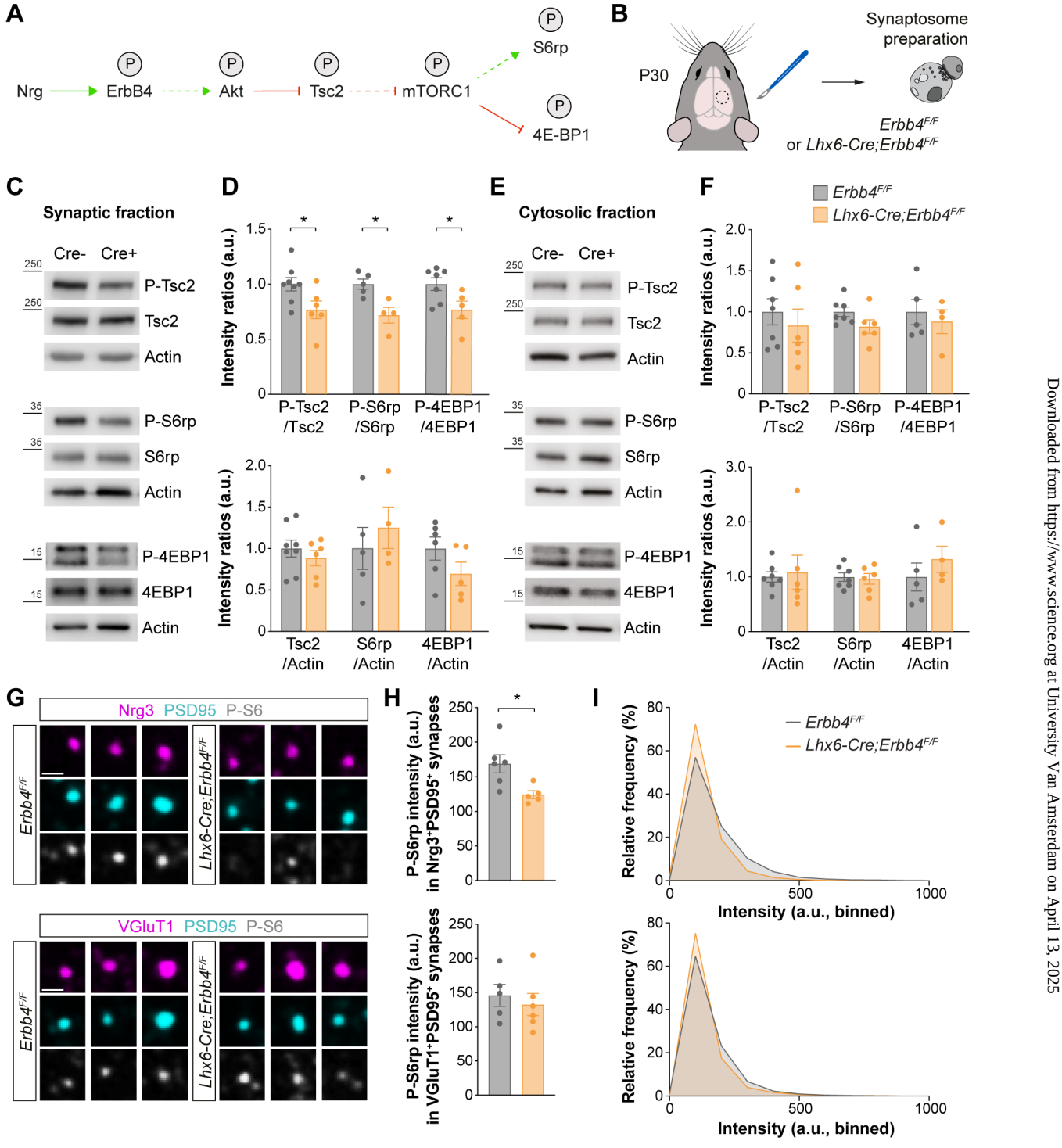

Fig. 2. ErbB4 regulates mTOR at excitatory synapses contacting PV$^+$ interneurons. (**A**) Hypothetical signaling pathway. P indicates phosphorylation; green arrow, activation; red arrow, inhibition; dotted arrows, indirect regulation. (**B**) Schematic of experimental design. (**C**) Phosphorylation and protein expression of Tsc2, S6rp, 4EBP1, and actin assessed by Western blot of cortical synaptic fractions from P30 homozygous conditional *Erbb4* mice and their control littermates. (**D**) Quantification of phosphorylation of Tsc2, S6rp, and 4EBP1 normalized to the total expression of the corresponding protein (top). Quantification of expression levels of Tsc2, S6rp, and 4EBP1 normalized to actin (bottom) (Tsc2: control, n = 8 mice, homozygous, n = 6 mice; S6rp: control, n = 5 mice, homozygous, n = 4 mice; 4EBP1: control, n = 7 mice, homozygous, n = 5 mice). (**E**) Phosphorylation and protein expression of Tsc2, S6rp, 4EBP1, and actin assessed by Western blot of cortical cytosolic fractions from P30 homozygous conditional *Erbb4* mice and their control littermates. (**F**) Quantification of phosphorylation of Tsc2, S6rp, and 4EBP1 normalized to the total expression of the corresponding protein (top). Quantification of expression levels of Tsc2, S6rp, and 4EBP1 normalized to actin (bottom) (Tsc2 and S6rp: control, n = 7 mice, homozygous, n = 6 mice; 4EBP1: control, n = 5 mice, homozygous, n = 4 mice). (**G**) Confocal images illustrating phosphorylation of S6rp (P-S6rp, gray) in Nrg3$^+$ (magenta) PSD95$^+$ (cyan)

synaptosomes (top) and in VGluT1$^+$ (magenta) PSD95$^+$ (cyan) synaptosomes (bottom) from P21 homozygous conditional *Erbb4* mice and their control littermates. (**H**) Quantification of P-S6rp staining intensity in Nrg3$^+$PSD95$^+$ (top) and VGluT1$^+$PSD95$^+$ synaptosomes (bottom). (**I**) Relative frequency distribution of P-S6rp staining intensity in Nrg3$^+$PSD95$^+$ synaptosomes (top) and in VGluT1$^+$PSD95$^+$ synaptosomes (bottom) (Nrg3$^+$PSD95$^+$: control, n = 22,063 synaptosomes from 6 mice, homozygous, n = 17,523 synaptosomes from 5 mice; VGluT1$^+$PSD95$^+$: control, n = 39,395 synaptosomes from 5 mice, homozygous, n = 48,057 synaptosomes from 6 mice). Two-tailed Student's unpaired t-tests: *P < 0.05. Data are mean ± SEM. Scale bar, 1 µm.

We confirmed that cortical PV$^+$ interneurons express these mRNAs during synaptogenesis (fig. S16, A and B) and that they are present in the dendrites of these cells (fig. S17; see also *24*). In addition, we found that these proteins cluster at the surface of PV$^+$ cells in close apposition to innervating axon terminals expressing the presynaptic ErbB4 ligand Nrg3 (fig. S16, C to E). Altogether, our data reveal dysregulation of postsynaptic molecular complexes in PV$^+$ cells lacking ErbB4.

ErbB4 regulates local protein synthesis at the synapse

Having identified ribosome-associated mRNAs that might be critical for the formation of excitatory synapses onto PV$^+$ cells, we next wondered whether ErbB4 might regulate this process by modulating the local translation of these transcripts. mTORC1 signaling is critical for the modulation of protein synthesis (*12*), and our previous results revealed that mTORC1 synaptic activity decreases in the absence of ErbB4 (Fig. 2). ErbB4 could therefore regulate synapse formation by controlling local protein synthesis at the synapse through the inhibition of Tsc2. To test this hypothesis, we assessed whether activation of ErbB4 signaling in cortical synaptosomes increases the translation of the ribosome-associated mRNAs we identified as down-regulated in *ErbB4* conditional mutants. To this end, we treated cortical synaptosomes with a soluble form of the epidermal growth factor (EGF)-like domain of neuregulin to activate ErbB4 receptors (*41*) (fig. S18, A to C) and examined candidate proteins by Western blot (Fig. 4A). We found increased protein levels for all but one of the downstream candidates of ErbB4 signaling (Fig. 4, B and C). We did not observe this increase when the samples were pretreated with the protein synthesis inhibitor cycloheximide (fig. S18, D and E), demonstrating that ErbB4 signaling induces the translation of these transcripts at the synapse. Altogether, these experiments revealed that ErbB4 regulates the local translation of synaptic proteins.

Mediators of excitatory synapse formation on PV$^+$ interneurons

To assess whether the proteins being synthesized downstream of ErbB4 are involved in the formation of excitatory synapses on cortical PV$^+$ interneurons, we performed interneuron-specific loss-of-function experiments in vivo using a conditional gene knockdown strategy (*42*). In brief, we designed conditional short-hairpin RNA vectors against the candidate genes (*shCadm1, shNptn, shNlgn3, shNtrk3, shClstn2, shGria4*, and *shCacng2*, with *shLacZ* as a control) and confirmed their effectiveness in vitro (fig. S19A). We generated adeno-associated viruses (AAVs) expressing

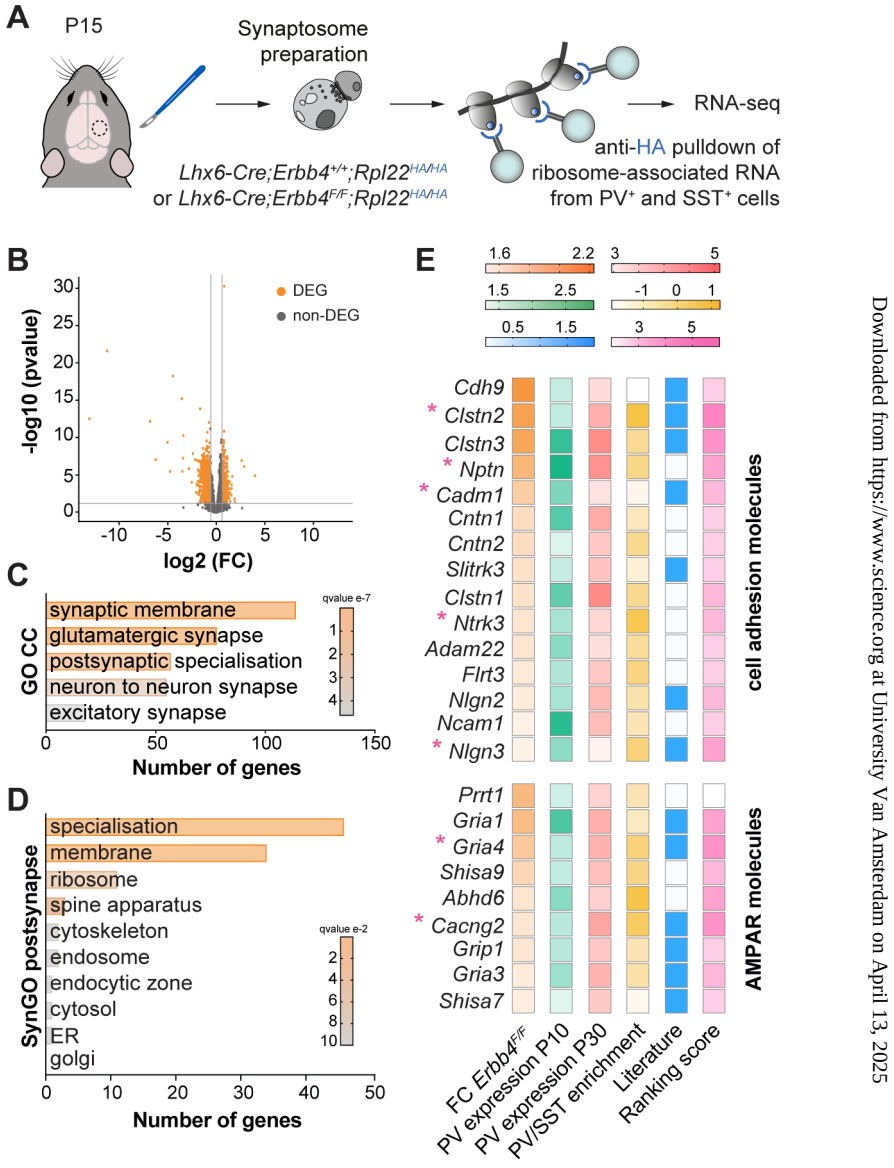

Fig. 3. Synaptic ribosome-associated mRNAs altered in *Erbb4* mutants. (**A**) Schematic of experimental design. (**B**) Volcano plot displaying significantly differentially expressed ribosome-associated RNAs (DEG, orange) in P15 cortical synaptosomes from homozygous conditional *Erbb4* mice compared with controls. Each dot represents one gene. FC, fold change (FC > 1.5, P < 0.05). (**C**) Selected gene ontology (GO) and cellular components (CC) terms significantly enriched in the dataset of downregulated genes in homozygous conditional *Erbb4* mutants compared with controls. (**D**) Synaptic gene ontology (SynGO) postsynaptic cellular component categories significantly enriched in the dataset of downregulated genes in homozygous conditional *Erbb4* mutants compared with controls. (**E**) Heatmaps showing the selection criteria for 15 "cell adhesion molecule" genes and 9 "AMPA receptor" genes. Asterisks indicate genes selected for validation.

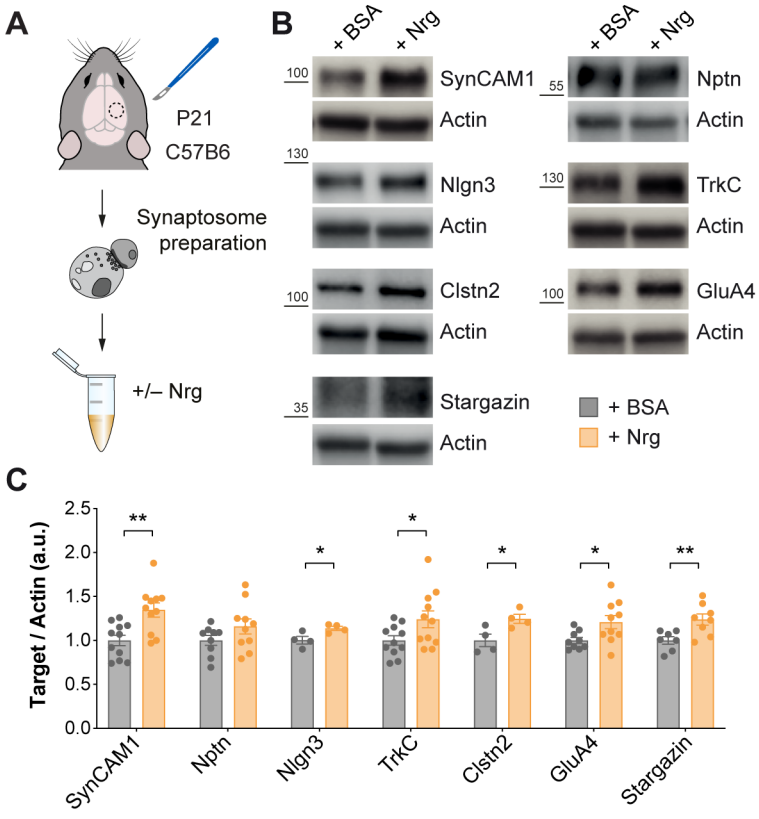

Fig. 4. ErbB4 regulates local translation of synaptic proteins. (**A**) Schematic of experimental design. (**B**) Protein expression of SynCAM1, Nptn, Nlgn3, TrkC, Clstn2, GluA4, Stargazin, and actin assessed by Western blot of cortical synaptic fractions treated with neuregulin (Nrg) from P21 C57B6 mice. (**C**) Quantification of expression levels of SynCAM1, Nptn, Nlgn3, TrkC, Clstn2, GluA4, and Stargazin normalized to actin. One-tailed Student's unpaired *t* tests: $*P < 0.05$, $**P < 0.01$ (SynCAM1 and TrkC: +BSA, n = 11 synaptosomes: +Nrg, n = 11 synaptosomes; Nptn and GluA4: +BSA, n = 9 synaptosomes, +Nrg, n = 10 synaptosomes; Nlgn3 and Clstn2: +BSA, n = 4 synaptosomes, +Nrg, n = 4 synaptosomes; Stargazin: +BSA, n = 7 synaptosomes, +Nrg, n = 8 synaptosomes). Data are mean ± SEM.

the most effective shRNA constructs, injected them into the neocortex of *Lhx6-Cre* neonates, and confirmed their ability to down-regulate the expression of the corresponding target genes in vivo (fig. S19B). We then assessed the number of excitatory synapses received by PV^+ interneurons expressing control and experimental *shRNAs* (Fig. 5A). We found that, compared with controls, reducing the expression of each of the seven targets in PV^+ interneurons led to a decrease in the density of excitatory synapses received by these cells (Fig. 5, B to D). These results revealed a complex molecular program regulated by ErbB4 that includes SynCAM1, Nlgn3, TrkC, Clstn2, GluA4, and Stargazin, and controls the formation of excitatory synapses onto PV^+ interneurons.

Discussion

Although local protein synthesis is common to synapses in the adult brain (*23*, *43*), the specificity of mRNA translation in different cell types and even in distinct connectivity motifs of the same neuron remains unexplored. Our work indicates that protein synthesis is regulated in a synapse type–specific manner during synapse formation. Tsc2, a regulator of mTORC1 signaling in multiple cellular contexts (*12*), regulates the development of excitatory synapses onto PV^+ cells but not onto SST^+ interneurons. This specificity is mediated by the activation of ErbB4, which controls excitatory synapse development through the inhibition of Tsc2 and the subsequent induction of a molecular program of mRNA translation involving the synthesis of several cell adhesion- and glutamate receptor-related proteins, including TrkC, Clstn2, GluA4, and Stargazin, as well as other molecules previously linked to glutamatergic synapses contacting interneurons (*44*–*46*). This synapse type–specific regulation could also involve a redistribution of the protein supply to neighboring maturing synapses, as described for synaptic plasticity (*47*).

Our results reveal that local translation is involved in synapse formation. Work in *Drosophila* suggested that the local action of the phosphatase Prl-1 (phosphatase of regenerating liver 1) in synapse formation might be achieved by local translation (*48*). Here, we found that translation occurs locally in developing synapses in the mammalian neocortex and that disrupting the machinery regulating protein synthesis deregulates synapse formation. Moreover, we demonstrate that many of the proteins identified as being synthesized at developing synapses are involved in synapse formation. Therefore, local translation contributes to brain wiring not only during axon guidance (*15*–*17*, *49*–*51*) but also in the final stages of neural circuit assembly.

Altered synthesis of synaptic proteins is a core pathophysiological mechanism in ASD (*52*–*57*). Although the evidence linking *ERBB4* with intellectual disability and ASD is scarce (*58*, *59*), the enrichment of autism-associated genes among the genes down-regulated in *ErbB4* conditional mutants and the identification of *NLGN3* as a target of ErbB4-Tsc2 signaling in the formation of excitatory synapses onto PV^+ interneurons is notable because mutations in *TSC2* and *NLGN3* are associated with ASD (*60*–*64*). The excitation received by PV^+ cells is modulated during experience (*42*, *65*, *66*), suggesting a prominent role in learning and memory. The synapse-specific molecular program unveiled in this study reinforces the idea that this connection is a sensitive hub for maladaptive network responses in neurodevelopmental disorders.

Materials and Methods summary

Conditional mouse mutants from MGE-derived interneurons were generated by crossing *Lhx6-Cre* mice with $Tsc2^{F/F}$ or $Erbb4^{F/F}$ mice. To generate cell type–specific knockdown in vivo, shRNAs against genes of interest were first tested for down-regulation in vitro. *Lhx6-Cre* neonates were then injected intracranially with Cre-dependent AAVs expressing the shRNAs with the highest knockdown efficiencies. For histological analyses, brains were fixed in 4% paraformaldehyde (PFA) and sectioned frozen on a sliding microtome (Leica). 40-μm thick sections were used for immunohistochemistry, whereas 30 μm thick sections were used to detect gene expression using the RNAscope Multiplex Fluorescent Assay protocol (ACDBio). Images were acquired with an inverted SP8 confocal microscope (Leica) or an ApoTome microscope (Zeiss) and analyzed with Imaris (Bitplane) and custom macros in FIJI (ImageJ). Synaptic function, paired-pulse ratio, and intrinsic properties of interneurons were analyzed by patch-clamp recordings on acute coronal slices using Mini Analysis (Synaptosoft) and Clampfit.

Synaptosomes were prepared with SynPER reagent (ThermoScientific) from cortical tissue and processed for several downstream

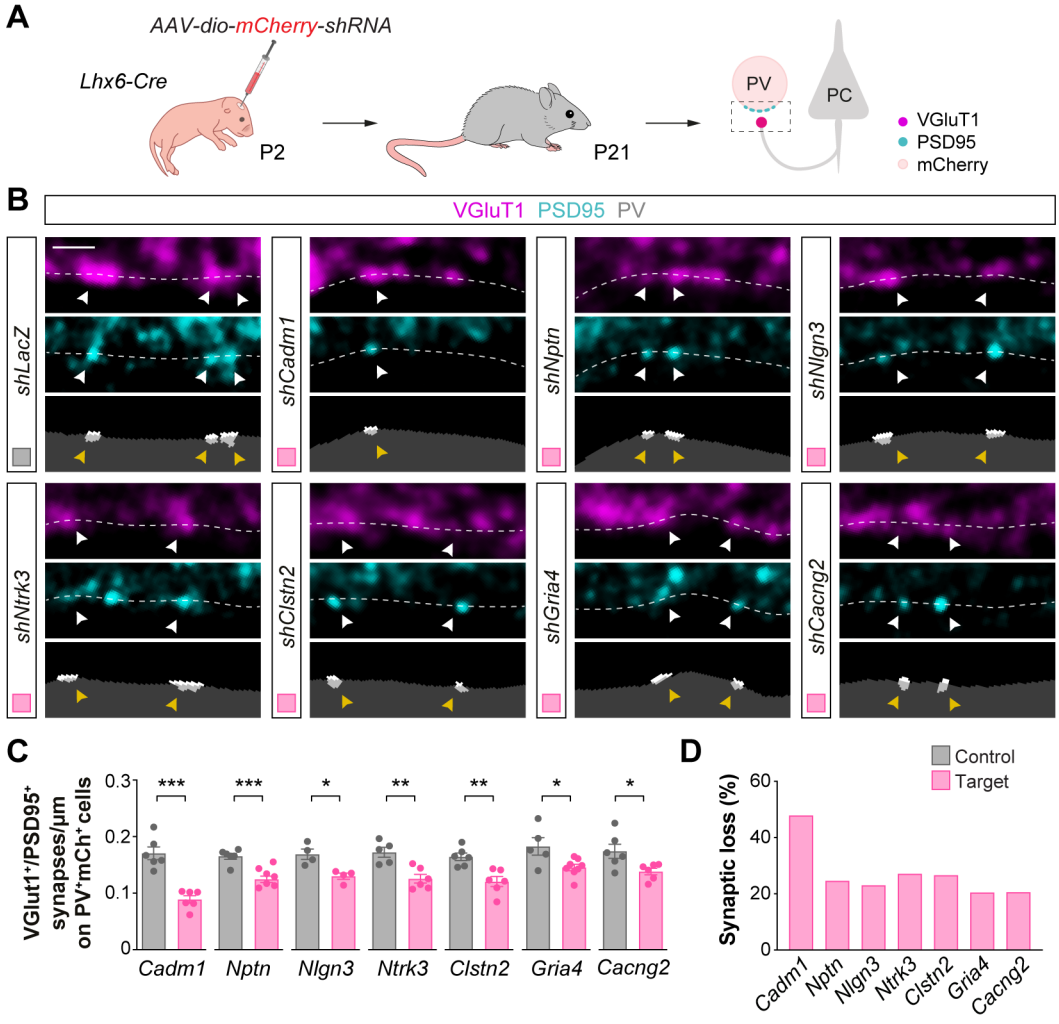

Fig. 5. ErbB4 targets control excitatory synapse formation on PV$^+$ interneurons. (**A**) Schematic of experimental design. (**B**) Confocal images (top) and binary images (bottom) illustrating presynaptic VGluT1$^+$ puncta (magenta) and postsynaptic PSD95$^+$ clusters (cyan) in PV$^+$ interneurons (gray) from P21 *Lhx6-Cre* mice injected with viruses expressing *shRNAs* targeting the genes of interest or with a control virus (*shLacZ*). (**C**) Quantification of the density of VGluT1$^+$PSD95$^+$ synapses contacting PV$^+$ interneurons in knockdown and control mice. Two-tailed Student's unpaired t-tests: *$P < 0.05$, **$P < 0.01$, ***$P < 0.001$; *shCadm1* (n = 122 cells from 6 mice) and control (n = 113 cells from 6 mice); *shNptn* (n = 131 cells from 6 mice) and control (n = 119 cells from 6 mice); *shNlgn3* (n = 86 cells from 4 mice) and control (n = 68 cells from 4 mice); *shNtrk3* (n = 126 cells from 6 mice) and control (n = 105 cells from 5 mice); *shClstn2* (n = 120 cells from 6 mice) and control (n = 112 cells from 6 mice); *shGria4* (n = 121 cells from 8 mice) and control (n = 93 cells from 5 mice); *shCacng2* (n = 115 cells from 6 mice) and control (n = 109 cells from 6 mice). (**D**) Proportion of synaptic loss in PV$^+$ interneurons upon knockdown of ErbB4 downstream targets. Data are mean ± SEM. Scale bar, 1 µm.

experiments, including coimmunoprecipitation, ErbB4 pathway activation and protein synthesis, Western blot, plating and immunofluorescence, and transmission electron microscopy. For coimmunoprecipitation, synaptosomes were incubated overnight with antibodies or isotype controls, added on Dynabeads (Invitrogen), and then extensively washed. For ErbB4 activation, synaptosomes were treated with Nrg-EGF or BSA for control, with or without pre-incubation with cycloheximide. For Western blot, denatured protein extracts were separated by SDS-PAGE and transferred onto PVDF membranes, blocked, and incubated with primary antibodies, HRP-conjugated secondary antibodies, and chemiluminescent substrates. Membranes were then imaged with an Odyssey FC (Li-Cor). Densitometry analyses were performed with Image Studio Lite. For immunofluorescence, synaptosomes were plated on 8-well chamber slides coated with poly-D-lysine and fixed with 4% PFA. Samples were then blocked and incubated overnight with primary antibodies, followed by washes and incubation with secondary antibodies for 2 hours at room temperature. For electron microscopy, synaptosomes were fixed in 2.5% glutaraldehyde. Following washes, postfixation, dehydration, and infiltration with Spurr epoxy resin-acetone mixture, samples were sectioned using an ultramicrotome (Leica) and examined on a JEM 1400 Flash transmission microscope (JEOL).

To isolate ribosome-associated RNAs of MGE-derived interneurons from cortical synaptic fractions, RiboTag (*Rpl22*$^{HA/HA}$) mice were crossed with *Lhx6-Cre;Erbb4*$^{F/F}$ mice. Following the preparation of synaptosomes and anti-HA pulldown using magnetic beads (Pierce), RNA samples were sequenced using a HiSeq 2500 platform (Illumina). Differential gene expression was performed using DESeq2 on R, and candidate targets were selected using the SynGO tool and ranked for validation using a set of criteria that included expression and enrichment in MGE-derived interneurons.

REFERENCES AND NOTES

1. T. Klausberger, P. Somogyi, Neuronal diversity and temporal dynamics: The unity of hippocampal circuit operations. *Science* **321**, 53–57 (2008). doi: 10.1126/science.1149381; pmid: 18599766
2. K. D. Harris, G. M. Shepherd, The neocortical circuit: Themes and variations. *Nat. Neurosci.* **18**, 170–181 (2015). doi: 10.1038/nn.3917; pmid: 25622573
3. R. J. Douglas, K. A. Martin, Neuronal circuits of the neocortex. *Annu. Rev. Neurosci.* **27**, 419–451 (2004). doi: 10.1146/annurev.neuro.27.070203.144152; pmid: 15217339
4. F. Ango *et al*., Ankyrin-based subcellular gradient of neurofascin, an immunoglobulin family protein, directs GABAergic innervation at purkinje axon initial segment. *Cell* **119**, 257–272 (2004). doi: 10.1016/j.cell.2004.10.004 pmid: 15479642
5. M. E. Williams *et al*., Cadherin-9 regulates synapse-specific differentiation in the developing hippocampus. *Neuron* **71**, 640–655 (2011). doi: 10.1016/j.neuron.2011.06.019 pmid: 21867881
6. X. Duan, A. Krishnaswamy, I. De la Huerta, J. R. Sanes, Type II cadherins guide assembly of a direction-selective retinal circuit. *Cell* **158**, 793–807 (2014). doi: 10.1016/j.cell.2014.06.047; pmid: 25126785
7. E. Favuzzi *et al*., Distinct molecular programs regulate synapse specificity in cortical inhibitory circuits. *Science* **363**, 413–417 (2019). doi: 10.1126/science.aau8977; pmid: 30679375
8. R. Sando, X. Jiang, T. C. Südhof, Latrophilin GPCRs direct synapse specificity by coincident binding of FLRTs and teneurins. *Science* **363**, eaav7969 (2019). doi: 10.1126/science.aav7969; pmid: 30792275
9. J. de Wit, A. Ghosh, Specification of synaptic connectivity by cell surface interactions. *Nat. Rev. Neurosci.* **17**, 22–35 (2016). doi: 10.1038/nrn.2015.3; pmid: 26656254
10. K. Shen, P. Scheiffele, Genetics and cell biology of building specific synaptic connectivity. *Annu. Rev. Neurosci.* **33**, 473–507 (2010). doi: 10.1146/annurev.neuro.051508.135302; pmid: 20367446
11. J. Pelletier, N. Sonenberg, The Organizing Principles of Eukaryotic Ribosome Recruitment. *Annu. Rev. Biochem.* **88**, 307–335 (2019). doi: 10.1146/annurev-biochem-013118-111042; pmid: 31220979
12. R. A. Saxton, D. M. Sabatini, mTOR signaling in growth, metabolism, and disease. *Cell* **168**, 960–976 (2017). doi: 10.1016/j.cell.2017.02.004; pmid: 28283069
13. X. Gao *et al*., Tsc tumour suppressor proteins antagonize amino-acid-TOR signalling. *Nat. Cell Biol.* **4**, 699–704 (2002). doi: 10.1038/ncb847; pmid: 12172555
14. K. Inoki, Y. Li, T. Zhu, J. Wu, K. L. Guan, TSC2 is phosphorylated and inhibited by Akt and suppresses mTOR signalling. *Nat. Cell Biol.* **4**, 648–657 (2002). doi: 10.1038/ncb839; pmid: 12172553
15. D. S. Campbell, C. E. Holt, Chemotropic responses of retinal growth cones mediated by rapid local protein synthesis and degradation. *Neuron* **32**, 1013–1026 (2001). doi: 10.1016/S0896-6273(01)00551-7; pmid: 11754834
16. P. A. Brittis, Q. Lu, J. G. Flanagan, Axonal protein synthesis provides a mechanism for localized regulation at an intermediate target. *Cell* **110**, 223–235 (2002). doi: 10.1016/S0092-8674(02)00813-9; pmid: 12150930
17. A. Poulopoulos *et al*., Subcellular transcriptomes and proteomes of developing axon projections in the cerebral cortex. *Nature* **565**, 356–360 (2019). doi: 10.1038/s41586-018-0847-y; pmid: 30626971
18. H. Kang, E. M. Schuman, A requirement for local protein synthesis in neurotrophin-induced hippocampal synaptic plasticity. *Science* **273**, 1402–1406 (1996). doi: 10.1126/science.273.5280.1402; pmid: 8703078
19. A. Gardiol, C. Racca, A. Triller, Dendritic and postsynaptic protein synthetic machinery. *J. Neurosci.* **19**, 168–179 (1999). doi: 10.1523/JNEUROSCI.19-01-00168.1999; pmid: 9870948
20. L. E. Ostroff, J. C. Fiala, B. Allwardt, K. M. Harris, Polyribosomes redistribute from dendritic shafts into spines with enlarged synapses during LTP in developing rat hippocampal slices. *Neuron* **35**, 535–545 (2002). doi: 10.1016/S0896-6273(02)00785-7; pmid: 12165474
21. S. J. Tang *et al*., A rapamycin-sensitive signaling pathway contributes to long-term synaptic plasticity in the hippocampus. *Proc. Natl. Acad. Sci. U.S.A.* **99**, 467–472 (2002). doi: 10.1073/pnas.012605299; pmid: 11756682
22. T. J. Younts *et al*., Presynaptic protein synthesis is required for long-term plasticity of GABA release. *Neuron* **92**, 479–492 (2016). doi: 10.1016/j.neuron.2016.09.040; pmid: 27764673
23. A. S. Hafner, P. G. Donlin-Asp, B. Leitch, E. Herzog, E. M. Schuman, Local protein synthesis is a ubiquitous feature of neuronal pre- and postsynaptic compartments. *Science* **364**, eaau3644 (2019). doi: 10.1126/science.aau3644; pmid: 31097639
24. J. D. Perez *et al*., Subcellular sequencing of single neurons reveals the dendritic transcriptome of GABAergic interneurons. *eLife* **10**, e63092 (2021). doi: 10.7554/eLife.63092; pmid: 33404500
25. L. Lim, D. Mi, A. Llorca, O. Marín, Development and functional diversification of cortical interneurons. *Neuron* **100**, 294–313 (2018). doi: 10.1016/j.neuron.2018.10.009; pmid: 30359598
26. A. Kepecs, G. Fishell, Interneuron cell types are fit to function. *Nature* **505**, 318–326 (2014). doi: 10.1038/nature12983 pmid: 24429630
27. D. C. Fingar, S. Salama, C. Tsou, E. Harlow, J. Blenis, Mammalian cell size is controlled by mTOR and its downstream targets S6K1 and 4EBP1/eIF4E. *Genes Dev.* **16**, 1472–1487 (2002). doi: 10.1101/gad.995802 pmid: 12080086
28. S. F. Tavazoie, V. A. Alvarez, D. A. Ridenour, D. J. Kwiatkowski, B. L. Sabatini, Regulation of neuronal morphology and function by the tumor suppressors Tsc1 and Tsc2. *Nat. Neurosci.* **8**, 1727–1734 (2005). doi: 10.1038/nn1566; pmid: 16286931
29. R. Malik *et al*., Tsc1 represses parvalbumin expression and fast-spiking properties in somatostatin lineage cortical interneurons. *Nat. Commun.* **10**, 4994 (2019). doi: 10.1038/s41467-019-12962-4; pmid: 31676823
30. J. P. Sommeijer, C. N. Levelt, Synaptotagmin-2 is a reliable marker for parvalbumin positive inhibitory boutons in the mouse visual cortex. *PLOS ONE* **7**, e35323 (2012). doi: 10.1371/journal.pone.0035323; pmid: 22539967
31. C. J. Potter, L. G. Pedraza, T. Xu, Akt regulates growth by directly phosphorylating Tsc2. *Nat. Cell Biol.* **4**, 658–665 (2002). doi: 10.1038/ncb840; pmid: 12172554
32. P. Fazzari *et al*., Control of cortical GABA circuitry development by Nrg1 and ErbB4 signalling. *Nature* **464**, 1376–1380 (2010). doi: 10.1038/nature08928; pmid: 20393464
33. A. K. Ting *et al*., Neuregulin 1 promotes excitatory synapse development and function in GABAergic interneurons. *J. Neurosci.* **31**, 15–25 (2011). doi: 10.1523/JNEUROSCI.2538-10.2011; pmid: 21209185
34. I. Del Pino *et al*., Erbb4 deletion from fast-spiking interneurons causes schizophrenia-like phenotypes. *Neuron* **79**, 1152–1168 (2013). doi: 10.1016/j.neuron.2013.07.010; pmid: 24050403
35. K. Elenius *et al*., Characterization of a naturally occurring ErbB4 isoform that does not bind or activate phosphatidyl inositol 3-kinase. *Oncogene* **18**, 2607–2615 (1999). doi: 10.1038/sj.onc.1202612; pmid: 10353604
36. D. Vullhorst *et al*., Selective expression of ErbB4 in interneurons, but not pyramidal cells, of the rodent hippocampus. *J. Neurosci.* **29**, 12255–12264 (2009). doi: 10.1523/JNEUROSCI.2454-09.2009; pmid: 19793984
37. T. Müller *et al*., Neuregulin 3 promotes excitatory synapse formation on hippocampal interneurons. *EMBO J.* **37**, 201798858 (2018). doi: 10.15252/embj.201798858 pmid: 30049711
38. D. Exposito-Alonso *et al*., Subcellular sorting of neuregulins controls the assembly of excitatory-inhibitory cortical circuits. *eLife* **9**, e57000 (2020). doi: 10.7554/eLife.57000 pmid: 33320083
39. E. Sanz *et al*., Cell-type-specific isolation of ribosome-associated mRNA from complex tissues. *Proc. Natl. Acad. Sci. U.S.A.* **106**, 13939–13944 (2009). doi: 10.1073/pnas.0907143106; pmid: 19666516
40. F. Koopmans *et al*., SynGO: An Evidence-Based, Expert-Curated Knowledge Base for the Synapse. *Neuron* **103**, 217–234.e4 (2019). doi: 10.1016/j.neuron.2019.05.002; pmid: 31171447
41. L. Mei, K. A. Nave, Neuregulin-ERBB signaling in the nervous system and neuropsychiatric diseases. *Neuron* **83**, 27–49 (2014). doi: 10.1016/j.neuron.2014.06.007; pmid: 24991953
42. E. Favuzzi *et al*., Activity-dependent gating of parvalbumin interneuron function by the perineuronal net protein Brevican. *Neuron* **95**, 639–655.e10 (2017). doi: 10.1016/j.neuron.2017.06.028; pmid: 28712654
43. J. D. Perez, C. M. Fusco, E. M. Schuman, A Functional Dissection of the mRNA and Locally Synthesized Protein Population in Neuronal Dendrites and Axons. *Annu. Rev. Genet.* **55**, 183–207 (2021). doi: 10.1146/annurev-genet-030321-054851; pmid: 34460296
44. J. S. Polepalli *et al*., Modulation of excitation on parvalbumin interneurons by neuroligin-3 regulates the hippocampal network. *Nat. Neurosci.* **20**, 219–229 (2017). doi: 10.1038/nn.4471; pmid: 28067903
45. K. A. Park *et al*., Excitatory Synaptic Drive and Feedforward Inhibition in the Hippocampal CA3 Circuit Are Regulated by SynCAM 1. *J. Neurosci.* **36**, 7464–7475 (2016). doi: 10.1523/JNEUROSCI.0189-16.2016; pmid: 27413156
46. A. Ribic, M. C. Crair, T. Biederer, Synapse-Selective Control of Cortical Maturation and Plasticity by Parvalbumin-Autonomous Action of SynCAM 1. *Cell Rep.* **26**, 381–393.e6 (2019). doi: 10.1016/j.celrep.2018.12.069 pmid: 30625321
47. C. Sun *et al*., The prevalence and specificity of local protein synthesis during neuronal synaptic plasticity. *Sci. Adv.* **7**, eabj0790 (2021). doi: 10.1126/sciadv.abj0790 pmid: 34533986
48. O. Urwyler *et al*., Branch-restricted localization of phosphatase Prl-1 specifies axonal synaptogenesis domains. *Science* **364**, eaau9952 (2019). doi: 10.1126/science.aau9952; pmid: 31048465
49. T. Shigeoka *et al*., Dynamic axonal translation in developing and mature visual circuits. *Cell* **166**, 181–192 (2016). doi: 10.1016/j.cell.2016.05.029; pmid: 27321671
50. T. Shigeoka *et al*., On-Site Ribosome Remodeling by Locally Synthesized Ribosomal Proteins in Axons. *Cell Rep.* **29**, 3605–3619.e10 (2019). doi: 10.1016/j.celrep.2019.11.025; pmid: 31825839
51. R. Cagnetta, C. K. Frese, T. Shigeoka, J. Krijgsveld, C. E. Holt, Rapid cue-specific remodeling of the nascent axonal proteome. *Neuron* **99**, 29–46.e4 (2018). doi: 10.1016/j.neuron.2018.06.004; pmid: 30008298
52. R. J. Kelleher 3rd, M. F. Bear, The autistic neuron: Troubled translation? *Cell* **135**, 401–406 (2008). doi: 10.1016/j.cell.2008.10.017; pmid: 18984149
53. M. Sahin, M. Sur, Genes, circuits, and precision therapies for autism and related neurodevelopmental disorders. *Science* **350**, aab3897 (2015). doi: 10.1126/science.aab3897; pmid: 26472761
54. C. Bagni, R. S. Zukin, A Synaptic Perspective of Fragile X Syndrome and Autism Spectrum Disorders. *Neuron* **101**, 1070–1088 (2019). doi: 10.1016/j.neuron.2019.02.041; pmid: 30897358
55. C. G. Gkogkas *et al*., Autism-related deficits via dysregulated eIF4E-dependent translational control. *Nature* **493**, 371–377 (2013). doi: 10.1038/nature11628; pmid: 23172145
56. E. Santini, E. Klann, Reciprocal signaling between translational control pathways and synaptic proteins in autism spectrum disorders. *Sci. Signal.* **7**, re10 (2014). doi: 10.1126/scisignal.2005832; pmid: 25351249
57. B. D. Auerbach, E. K. Osterweil, M. F. Bear, Mutations causing syndromic autism define an axis of synaptic pathophysiology. *Nature* **480**, 63–68 (2011). doi: 10.1038/nature10658; pmid: 22113615
58. J. Kasnauskiene *et al*., A new single gene deletion on 2q34: ERBB4 is associated with intellectual disability. *Am. J. Med. Genet. A.* **161A**, 1487–1490 (2013). doi: 10.1002/ajmg.a.35911; pmid: 23633123
59. A. B. Wilfert *et al*., Recent ultra-rare inherited variants implicate new autism candidate risk genes. *Nat. Genet.* **53**, 1125–1134 (2021). doi: 10.1038/s41588-021-00899-8 pmid: 34312540
60. P. J. de Vries *et al*., Tuberous sclerosis associated neuropsychiatric disorders (TAND) and the TAND Checklist. *Pediatr. Neurol.* **52**, 25–35 (2015). doi: 10.1016/j.pediatrneurol.2014.10.004; pmid: 25532776
61. C. L. Salussolia, K. Klonowska, D. J. Kwiatkowski, M. Sahin, Genetic Etiologies, Diagnosis, and Treatment of Tuberous Sclerosis Complex. *Annu. Rev. Genomics Hum. Genet.* **20**, 217–240 (2019). doi: 10.1146/annurev-genom-083118-015354; pmid: 31018109
62. K. D. Winden, D. Ebrahimi-Fakhari, M. Sahin, Abnormal mTOR Activation in Autism. *Annu. Rev. Neurosci.* **41**, 1–23 (2018). doi: 10.1146/annurev-neuro-080317-061747 pmid: 29490194
63. S. Jamain *et al*., Mutations of the X-linked genes encoding neuroligins NLGN3 and NLGN4 are associated with autism. *Nat. Genet.* **34**, 27–29 (2003). doi: 10.1038/ng1136 pmid: 12669065
64. S. J. Sanders *et al*., Insights into autism spectrum disorder genomic architecture and biology from 71 risk loci. *Neuron* **87**, 1215–1233 (2015). doi: 10.1016/j.neuron.2015.09.016; pmid: 26402605
65. F. Donato, S. B. Rompani, P. Caroni, Parvalbumin-expressing basket-cell network plasticity induced by experience regulates

adult learning. *Nature* **504**, 272–276 (2013). doi: 10.1038/nature12866; pmid: 24336286
66. N. Dehorter *et al*., Tuning of fast-spiking interneuron properties by an activity-dependent transcriptional switch. *Science* **349**, 1216–1220 (2015). doi: 10.1126/science.aab3415; pmid: 26359400

ACKNOWLEDGMENTS

We thank T. Garcés and E. Serafeimidou-Pouliou for general laboratory support, I. Andrew for managing mouse colonies, the Centre for Genomic Regulation (CRG) Genomics Unit for RNA-seq, P. de la Grange at GenoSplice for help with bioinformatic analyses, and P. Machado at the Centre for Ultrastructural Imaging for help with electron microscopy analysis. We are also grateful to J. Bateman, M.J. Conde-Dusman, G. Condomitti, N. Flames, and C. Houart for critical reading of the manuscript and members of the Marín and Rico laboratories for stimulating discussions and ideas. **Funding:** This work was supported by grants from the Innovative Medicines Initiative 2 Joint Undertaking grant agreement 777394 for the project AIMS-2-TRIALS and the Simons Foundation Autism Research Initiative (SFARI) grant 736666 to B.R. and O.M. The IMI2 Joint Undertaking receives support from the European Union's Horizon 2020 research and innovation program, EFPIA, Autism Speaks, Autistica, and SFARI. The funders had no role in the design of the study; in the collection, analyses, or interpretation of data; in the writing of the manuscript, or in the decision to publish the results. Any views expressed are those of the author(s) and not necessarily those of the funders. For the purpose of open access, the authors have applied a CC BY public copyright license to any Author Accepted Manuscript version arising from this submission. **Author contributions:** C.B., D.E-A., M.S., B.R., and O.M. designed experiments. C.B. carried out the biochemical experiments and the histological analysis of the *Tsc2* mutants. M.S. performed electrophysiological experiments. D.E-A. performed the functional analysis of target genes. A.A., A.H-G., and S.S. contributed to data collection and analysis. F.O. and P.M. produced the AAVs. F.H. performed the SFARI gene enrichment analysis. L.A., M.R., and R.F. prepared and imaged the electron microscopy samples. C.B., B.R., and O.M. wrote the manuscript with input from all authors. **Competing interests:** The authors declare no competing interests. **Data and materials availability:** Sequencing data have been deposited at the National Center for Biotechnology Information BioProjects Gene Expression Omnibus (GEO) and are accessible through GEO Series accession number GSE214258. All other data are available in the manuscript or the supplementary material.

SUPPLEMENTARY MATERIALS

science.org/doi/10.1126/science.abm7466
Materials and Methods
Figs. S1 to S19
Table S1
References (*67*–*75*)
MDAR Reproducibility Checklist

View/request a protocol for this paper from *Bio-protocol*.

Submitted 15 June 2022; accepted 17 October 2022
10.1126/science.abm7466